



Influences of nano zero valent iron and Fe²⁺ supported kaolin nanoparticles for metal ion separation thorough ultrafiltration

K. Thiyagarajan^a, G. Arthanareeswaran^{a,*}, Jihyang Kweon^b, Diganta B. Das^c, V. Jaikumar^d

^aMembrane Research Laboratory, Department of Chemical Engineering, National Institute of Technology, Tiruchirappalli 620015, India, email: skthiyagaraj@gmail.com (K. Thiyagarajan), Tel. +91431-2503118, Fax +91431-2500133, email: arthanaree10@yahoo.com (G. Arthanareeswaran)

^bWater Treatment and Membrane Laboratory, Department of Environmental Engineering, Konkuk University, Seoul 05029, Republic of Korea, email: jhkweon@konkuk.ac.kr (J. Kweon)

^cDepartment of Chemical Engineering, Loughborough University, Loughborough LE11 3TU, UK, email: D.B.Das@lboro.ac.uk (D.B. Das)

^dDepartment of Chemical Engineering, SSN College of Engineering, Chennai 603 110, India, email: jaikumaru@ssn.edu.in (V. Jaikumar)

Received 27 September 2018; Accepted 9 March 2019

ABSTRACT

In this work, clay based nanocomposite material was synthesized by wet chemical route and nano-zero valent iron of kaolin (nZVI:Kaolin) were prepared using sodium borohydride reduction method. The nZVI:Kaolin and Fe:Kaolin nanoparticles were characterized using XRD, FTIR, SEM and antimicrobial activity. The nZVI:Kaolin and Fe:Kaolin were incorporated into polyethersulfone (PES) membranes for metal ion separation through ultrafiltration. The influences of nZVI:Kaolin and Fe supported clay nanoparticles on PES membranes were characterized their modification in functional properties, hydrophilicity and morphological structure. The clean water flux was enhanced to PES membrane by addition of nZVI:Kaolin and Fe:Kaolin nanoparticles. The Cu(II), Ni(II) and Cd(II) metal ions flux was increased for 0.15 wt% of nZVI and Fe:Kaolin nanoparticles in PES which is due to increase in hydrophilicity and change in morphological structure.

Keywords: Metal ion separation; Clay nanomaterials; nZVI:Kaolin; Membrane morphology; Permeate flux

1. Introduction

Polymers are widely used for membrane fabrication in wastewater treatment applications such as ultrafiltration (UF) and reverse osmosis (RO). The polymer membranes are serviced as asymmetric barrier to separate macromolecules with applied pressure in ultrafiltration process [1]. The solution casting method is a well-known technique to develop asymmetric structure of polymer membranes [2]. The developed asymmetric membrane having dense top layer and a porous sub-layer for the separation molecular, macromolecular and ionic molecules [2]. Polyethersulfone (PES) is having superior membrane properties in metal ions separation, however, it is having inherent hydrophobicity

and low flux. Hence, modification of hydrophobicity and flux enhancement is needed for metal ion separation [3]. The modification by simple physical blending of polymer with inorganic materials for membrane formation has attracted due to interconnectivity and covalent bonding and properties enhancement of inorganics [4–8]. For example, the inorganic materials of silica [9], zirconium dioxide (ZrO₂), [10] Al₂O₃ [11], lithium salts [12], have been blended with polyvinylidene fluoride (PVDF) and have been applied for wastewater treatment.

In recent years, the use of clay nanocomposites in polymer/clay nanocomposites (PCN) with low clay loading are the benefit to promote better dispersion [13,14] and used for membrane application [15]. In our previous study, PAN/nanokaolinite membranes have been appeared to have

*Corresponding author.

Presented at the InDA Conference 2018 (InDA CON-2018), 20–21 April 2018, Tiruchirappalli, India

improvement in colour removal during textile wastewater treatment [16]. Monticelli et al. reported that clay minerals have been improved mechanical and thermal properties of polymer nanocomposite membranes [17]. Blending of polymer with inorganic clay minerals has resulted in new class materials which are nanocomposite structure, with the complete dispersion of clay mineral in the polymer matrix, adsorbed solutes on the surface or interpolated in the inter-layer spaces of the clay [18,19]. The clay minerals are more active in polymer membrane modification such as to create large surface area in polymer network with nano-scale and strong electrostatic interactions on surface [20].

The distribution zero valent ions (nZVI) in nanomaterials TiO_2 matrix showed good removal of hexavalent chromium, Cr(VI) in wastewater [21]. The capability of reduction of Cu(II) to Cu(I), and inhibit oxidation of ZVI from Fe^0 to Fe^{3+} of ZVI in hybrid polysulfone/ZVI membranes was demonstrated [22]. In this work, dispersion of ZVI particles in both inside the pores and their surface was also reported [22]. According to literatures, the main advantages of zero valent ions present in clay are reduction and removal efficiency metal ion from industry wastewater. Liu et al. investigated the effect of highly porous chitosan (CS) in cellulose acetate (CA) for removal of copper ion from aqueous solutions [23]. Kaşgöz et al. synthesized clay particles and incorporated on the acrylamide (AAm)-2-acrylamido-2-methylpropane sulfonic acid (AMPS) polymers for effective removal of Cu(II), Cd(II), and Pb(II) from aqueous solution [24]. From their investigation, low loading of clay minerals into the polymer was influenced the removal of heavy metal ion. The different compositions of activated bentonite clay were incorporated into polyetherimide membranes and bentonite clay showed an enhancement in porosity, hydrophilicity [25]. The addition of bentonite clay improved the permeate flux and rejection of Cu(II), Ni(II) and Cd(II) ions. The clay plays as major role in effective removal of metal ions by affinity of metal ions on membrane surface and increased adsorption capacity. Hence, clay-nZVI composite is used as inorganic modifier for effective application of polyethersulfone membranes in metal ion removal. In our study, the effect of nZVI and Fe supported clay particles on removal capacity of Cu(II), Ni(II) and Cd(II) ions solution in PES membranes

2. Experimental

2.1. Materials and methods

Kaolin clay was purchased from Loba chemicals (Mumbai-India). Ferric chloride (FeCl_3), reducing agent (NaBH_4) is purchased from Merck India. Polyethersulfone (PES) was purchased from Solvay specialites India Ltd. N, N'- dimethylformamide (DMF) and sodium lauryl sulfate (SLS) were obtained from Qualigens Fine Chemicals Ltd. Polyethyleneimine (molecular weight = 25,000 g/mol) was procured from Fluka, Germany. Copper sulfate, nickel sulfate and cadmium sulfate were procured from Merck (India) Ltd.

2.2. Synthesis of nZVI-Kaolin nanocomposite

The synthesis of nano zerovalent iron:Kaolin (nZVI:Kaolin) was synthesized by borohydride reduction method

[26]. The 4.86 g of FeCl_3 was dissolved in a 4/1 (v/v) ethanol/water mixture. Then 1 g of kaolinite was added to the mixture and the mixture was left in an ultrasonic bath for 30 min in order to obtain complete dispersion of kaolinite grains. Meanwhile, 1.0 M sodium borohydride solution was prepared by dissolving 3.78 g NaBH_4 in 100 mL of water. The borohydride solution was then added drop wise to the aqueous FeCl_3 and kaolinite mixture while stirring at the speed of 600 rpm. The excess borohydride is used for the complete reduction of Fe^{3+} ions. The black solid particles of nZVI appeared immediately following the addition of the first drop of NaBH_4 solution its shows the formation of iron particles. After the complete addition of the borohydride solution, the mixture was left 6 h for stirring. The nZVI:Kaolin solution mixture was centrifuged and rinsed with EtOH and dried under vacuum for 3h at 80°C .

2.3. Synthesis of Fe^{2+} supported kaolin nanoparticles

The clay supported Fe^{2+} supported kaolin nanoparticles (Fe:Kaolin) was synthesized by wet chemical route method. The 1 g of kaolin powder was mixed with the 20 mL of Millipore water and left in the ultrasonicator bath for 30 min in order to disperse the kaolin grains. 1 g of cetrimide (CTAB) was added to the solution mixture as chelating agent to prevent the agglomeration of the metal nanoparticles. 0.1 M concentration of metal precursors solution was prepared by dissolving the FeCl_3 , $\text{Co}(\text{NO}_3)_2 \cdot 6\text{H}_2\text{O}$, $\text{NiSO}_4 \cdot 6\text{H}_2\text{O}$, and $\text{FeSO}_4 \cdot 7\text{H}_2\text{O}$ each in 10 mL of water. The metal precursor solutions were added one by one into the solution mixture for 30 min interval at constant stirrer speed of 500 rpm [27]. 1.0 M sodiumborohydride (NaBH_4) solution was prepared by dissolving 3.78 g in 100 mL of water. The water is added drop wise to the above solution mixture at vigorous stirring. While adding the NaBH_4 , the changes in color showed formation of nanoparticles. After complete addition of NaBH_4 , the mixture was stirred for 12 h and washed with ethanol for several times to remove the by-product from the nanocomposites.

2.4. Preparation of clay/polymer nanocomposite membranes

The nZVI:Kaolin and Fe:Kaolin were dispersed well in dimethylformamide (DMF) individually by sonication under in an ultrasonication bath maintained at 30°C for 15 min. The formulation of PES, nZVI:Kaolin and Fe:Kaolin is provided in Table 1. The dispersed nZVI:Kaolin and Fe:Kaolin in solvent mixture was then mixed with PES for 3h mechanical stirrer at 50°C to get homogeneous dope solution. The mixed nZVI:Kaolin/PES and Fe:Kaolin/PES dope solution were again ultrasonicated for 40 min for finishing the dispersion of both nZVI:Kaolin and Fe:Kaolin nanoparticles in individual PES. The addition of nZVI:Kaolin and Fe:Kaolin beyond 0.03 g in PES was showed heterogeneous and turbid in dope solution. Further, we found that phase separation and defects during membrane formation at above 0.03 g of nZVI:Kaolin and Fe:Kaolin in PES. Hence, 0.015 and 0.030 g of nZVI:Kaolin and Fe:Kaolin were selected for modification of PES membrane. Then the dope solution was then degassed and cooled at 25°C . The solution was cast on a

Table 1
Membrane compositions and contact angle of PES membranes

PES (g)	Membrane name	Clay nanoparticles (g)		DMF (ml)	Contact angle (°)
		nZVI:Kaolin	Fe:Kaolin		
4.380	PES	–	–	21.7	82
4.365	PES-Z1	0.015	–	21.7	74
4.350	PES-Z2	0.030	–	21.7	78
4.365	PES-F1	–	0.015	21.7	72
4.350	PES-F3	–	0.030	21.7	65

clean glass plate using a thin film applicator. The thickness was kept uniformly at 400 μm and temperature of casting chamber was maintained at $20 \pm 2^\circ\text{C}$ and relative humidity of 50%. The cast membranes were immersed in the gelation bath, the membranes were washed after 3 h and stored.

2.5. Characterization of nZVI:Kaolin, Fe:Kaolin nanoparticles, nZVI:Kaolin/PES and Fe:Kaolin/PES membranes

X-ray diffraction patterns of the nZVI:Kaolin and Fe:Kaolin, nZVI:Kaolin/PES membranes and Fe:Kaolin/PES membranes were analyzed by Rigaku III Dmax 2500 diffractometer using Cu KR radiation. The diffractograms were obtained at the scattering angles from $10\text{--}80^\circ$ for 30 min at a scanning rate of $2^\circ/\text{min}$. The elemental analysis of nZVI:Kaolin nanocomposites, Fe:Kaolin, nZVI:Kaolin/PES membranes and Fe:Kaolin/PES membranes were studied using FTIR (in KBr) spectra were determined with help of PerkinElmer Spectrum RX-I spectroscope (Perkin Elmer Instruments, Buckinghamshire, UK). Contact angle measurements were conducted on a Rame-Hart goniometer (Rame-Hart Instrument Co., Succasunna, NJ, USA). A small drop of water was placed on the top surface of the polymer membrane surface using a micro syringe and the contact angle was measured at a constant time interval at the various places of the membrane. The morphological study of kaolin nanocomposites, Fe:Kaolin, nZVI:Kaolin/PES membranes and Fe:Kaolin/PES membranes were studied using scanning electron microscopy (SEM) (Hitachi S-3000H).

2.6. Antimicrobial activity

The antimicrobial activity of the nZVI:Kaolin and Fe:Kaolin were carried out on the basis of standard antibiotic susceptibility test using *Staphylococcus aureus* and *Klebsiella pneumonia* by Kirby-Bauer method. The Muller Hinton agar was inoculated with ten microliters of the overnight cultures of *Staphylococcus aureus* and *Klebsiella pneumonia*. A sterile swab was dipped into this culture and used to inoculate the surface of a fresh Mueller Hinton agar plates and were allowed to dry for 2–5 min. The antibiotics disc and the plant sample discs at different concentration were spaced out onto the plates and were incubated at 37°C for 24 h. The diameter of the clear zone and each plant sample discs were determined.

3. Permeation properties

3.1. Pure water flux

Water flux studies were carried out using model Cell-XFUF076, Millipore, USA for all nanocomposite membranes under 60 psi with membrane effective surface area of 38.5 cm^2 at 25°C . The water flux (J_w) calculated using the following equation:

$$J_w = \frac{Q}{A \cdot \Delta T} \quad (1)$$

where J_w is the permeate flux, $\text{l m}^{-2}\text{ h}^{-1}$; Q is the quantity of permeate, l ; A is the membrane area, m^2 ; ΔT is the sampling time, h .

3.2. Metal ion separation studies

The Cu(II), Ni(II) and Cd(II) were synthesized at a concentration of 1000 ppm in 1 wt.% solution of PEI and rejection and permeation of nZVI:Kaolin and Fe:Kaolin incorporated PES membrane were carried in UF stirred dead end cell. The pH was maintained to 7 to avoid any precipitation of metal ions. The concentrations of the feed and permeate of the metal ions was analysed using an atomic absorption spectrophotometer (Perkin-Elmer 3110). The percentage rejections of metal ions were calculated using Eq. (2)

$$\%SR = \left[1 - \left(\frac{C_p}{C_f} \right) \right] \times 100 \quad (2)$$

where C_p is the concentration of permeate, and C_f is the concentration feed.

4. Results and discussion

4.1. Characterization of nZVI:Kaolin and Fe:Kaolin nanoparticles

4.1.1. XRD-analysis

The XRD pattern of nZVI:Kaolin is provided in Fig. 1. In this XRD pattern, the broad peak exposes the presence of an amorphous phase of iron. The characteristic broad peak at 2θ of 45° indicates that the zero-valent iron is predominantly present in nanoparticles [28]. The clay peaks are shifted towards the higher value of 2θ . The appeared peak at 2θ of 56.55° is because of the formation of SiO_2 . Fig. 1 shows the XRD pattern of the clay supported Fe nanoparticles. The XRD pattern for the metal kaolin was shows the same pattern with the virgin kaolin. The small intensity change at 2θ value of 30.62 is appeared for Fe ion in the plane of (2:1:1) present in clay supported Fe nanoparticles. The other metals are not showing any peak due to the more interaction of clay microcavity ion and the metal ions present in nanomaterials. Another reason for the no peak formation is the low concentration of metal ions compare to the kaolin (0.1:1). The average particle size of the nZVI:Kaolin nanocomposites was 42 nm which is calculated by Scherrer formula [28].

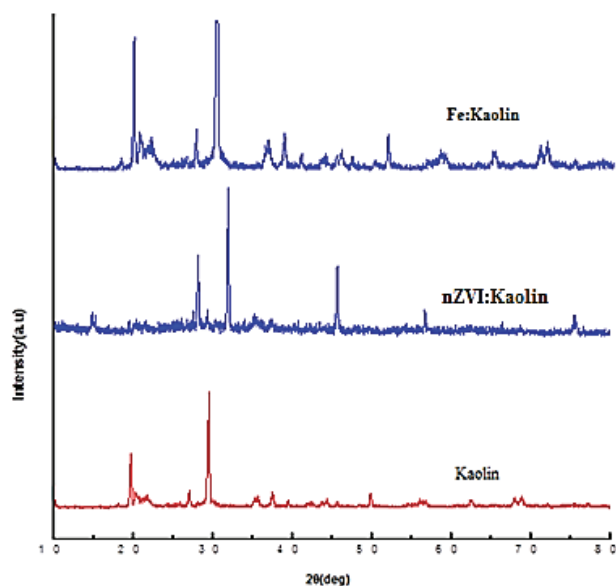


Fig. 1. XRD-pattern for the kaolin, nZVI:Kaolin and Fe:Kaolin nanoparticles.

4.1.2. FT-IR analysis

The elemental analysis of nZVI:Kaolin and Fe:Kaolin nanoparticles were studied by apply scan between 4000 cm^{-1} to 400 cm^{-1} . As shown in Fig. 2, the peak at the wave-number 694 cm^{-1} is due to deformation of Al-O-Si stretching of the clay materials [29]. The peak at the 826 cm^{-1} shows that the deformation of OH- stretching. The broad peak at $1566\text{--}1628\text{ cm}^{-1}$ due to the stretching of the Fe-O-water. The wave number 2352 cm^{-1} shows the asymmetric stretching of -OH group in the composite materials [29]. Broad bands observed around 3500 cm^{-1} due to the water absorbed during palletisation [30]. All the other peaks present in the spectrum are corresponding to the base materials.

4.1.3. Morphology

Figs. 3 and 4 show the SEM images of nZVI:Kaolin, and Fe:Kaolin nanoparticles. Fig. 3 shows that nZVI:Kaolin nanoparticles with a diameter about 25–45 nm distributed on the kaolinite [31]. As shown in Fig. 4, Fe size was increased and covered on the surface after reaction of iron oxide in kaolin aqueous solution. This is attributed to the formation of iron oxide precursors on the surface of nanoparticles [32]. The image shows that Fe nanoparticles were dispersed on the surface and edges of kaolinite. The clay mineral appeared at the edge sites and contain more nanoparticles in comparison to the surface of virgin PES membrane.

4.1.4. Antimicrobial activity

The antimicrobial activity of the nZVI:Kaolin and Fe:Kaolin was tested against two bacterial species. The zones of inhibition measured for control and nZVI:Kaolin and Fe:Kaolin against the model organisms is shown in Fig. 5. The nZVI:Kaolin nanocomposites showed more

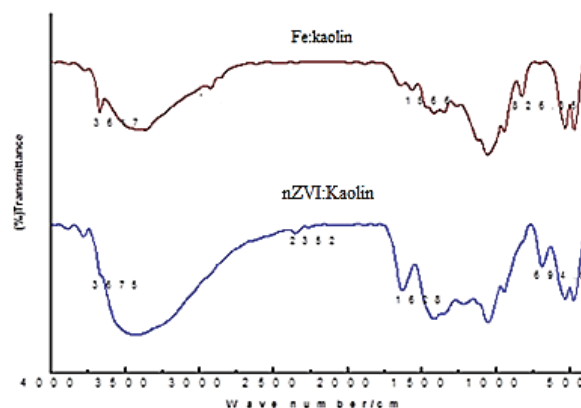


Fig. 2. FTIR spectra of nZVI:Kaolin and Fe:Kaolin nanoparticles.

activity against the bacterial species *Staphylococcus aureus* when compared to *Klebsiella pneumoniae*. Fe:Kaolin only small zone against the bacterial species. Wu et al. [33] studied the antimicrobial properties and influence factors of clay minerals and concluded that control clays have no antimicrobial ability, however, the modified clay minerals significantly inhibited the growth of bacteria. The diameter of the inhibition zones was increased in addition of nZVI, and Fe on clay membrane. This is confirmed that nZVI:Kaolin and Fe:Kaolin influenced the antimicrobial activity of nZVI:Kaolin/PES and Fe:Kaolin/PES on the membrane surface.

4.2. Characterization of nZVI:Kaolin and Fe:Kaolin incorporated PES polymer membrane

4.2.1. XRD analysis

X-ray diffraction patterns of PES membrane with nZVI:Kaolin and clay supported metallic Fe nanoparticles is shown in Fig. 6. From the XRD pattern of the composite membrane there is no intensity variation peak for metal present in the clay material. For nZVI:Kaolin/PES membrane, XRD pattern is similar to the PES membrane. However, Fe:Kaolin/PES membrane, the slight variation in the intensity at the 2θ value of 29.21 was observed by incorporation metal Fe in kaolinite. The behavior from Fig. 6 may represent an interlay of aluminosilicate particles in polymer (PES) through the distribution of Fe metal was confirmed.

4.2.2. FT-IR analysis

From Fig. 7, the strong peak at 1658 and 1666 cm^{-1} are associated with the C-H₂ bending vibration respectively. The symmetrical and asymmetrical stretching vibrations for the pure PES appeared for aromatic ether (-C-O-C-) linkages hit the peak at 1241 cm^{-1} and peaks at the 1481 and 1581 cm^{-1} are assigned to the aromatic benzene ring [34]. The FTIR spectrum showed that a strong peak at 1711 cm^{-1} assigned to asymmetric stretching of carboxyl groups emerged for PES membrane matrix. The appearance of carboxyl groups was remarkably confirmed the addition of nZVI:Kaolin. However, clay supported metallic Fe nanoparticles were incor-

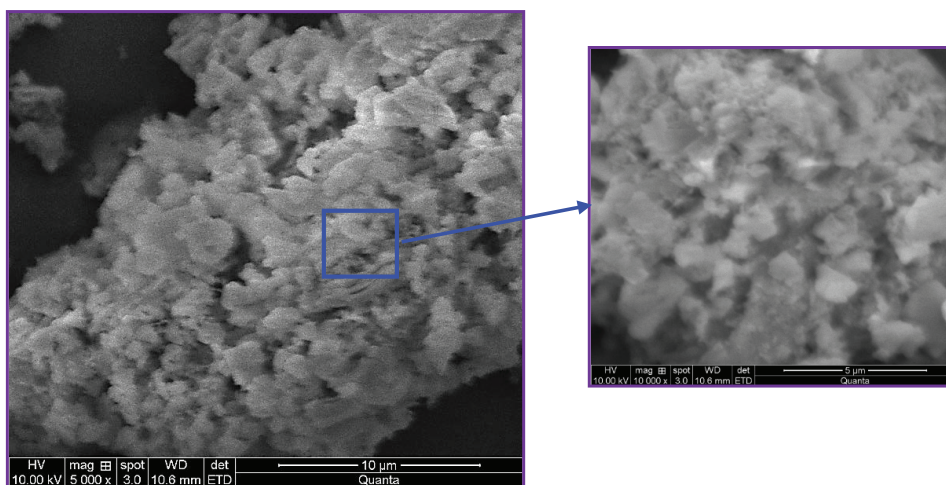


Fig. 3. Morphology of nZVI:Kaolin nanoparticles.

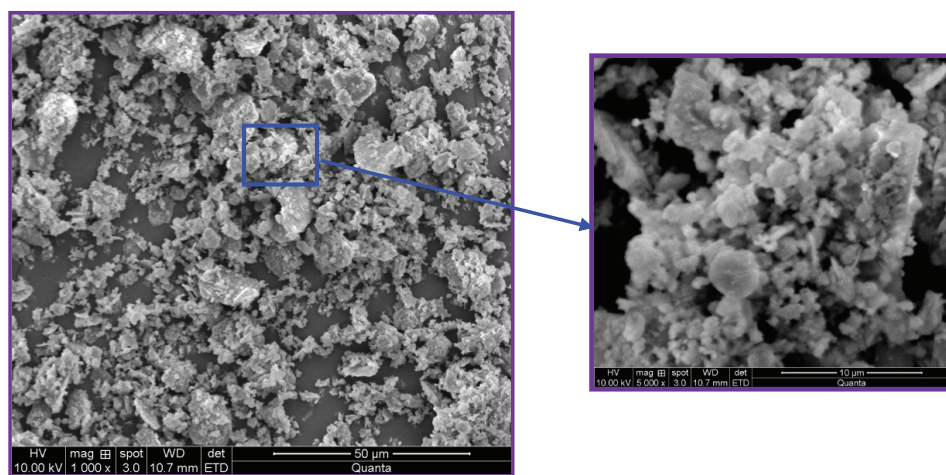


Fig. 4. Morphology of Fe:Kaolin nanoparticles.

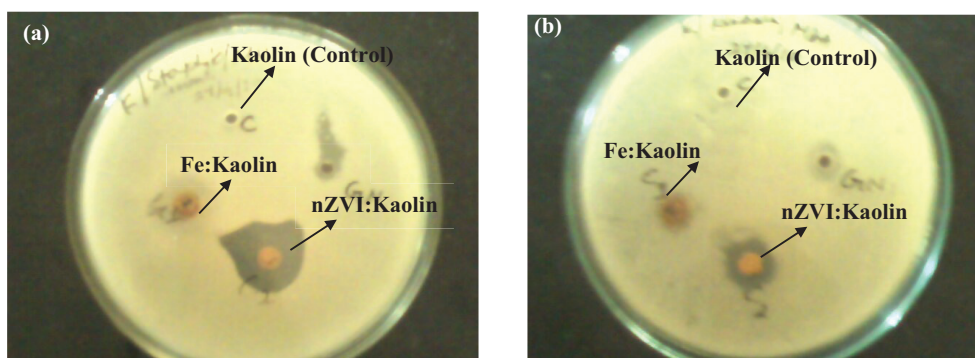


Fig. 5. Antimicrobial activity of Kaolin, nZVI:Kaolin and Fe:Kaolin nanoparticles against the (a) *Staphylococcus aureus* (b) *Klebsiella pneumoniae*.

porated in PES membrane, the peak intensity of carboxyl groups decreased. This suggested that significant interactions may be ensure between nZVI:Kaolin, Fe:Kaolin and carboxyl groups [35].

4.2.3. Morphological structure

The surface and cross-sectional morphology of nZVI:Kaolin/PES and Fe:Kaolin/PES membranes

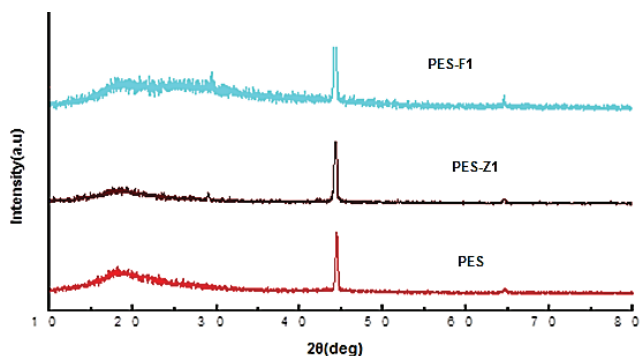


Fig. 6. XRD pattern of PES, PES, nZVI:Kaolin/PES (0.015 wt.%) and Fe:Kaolin/PES (0.015 wt.%) membranes.

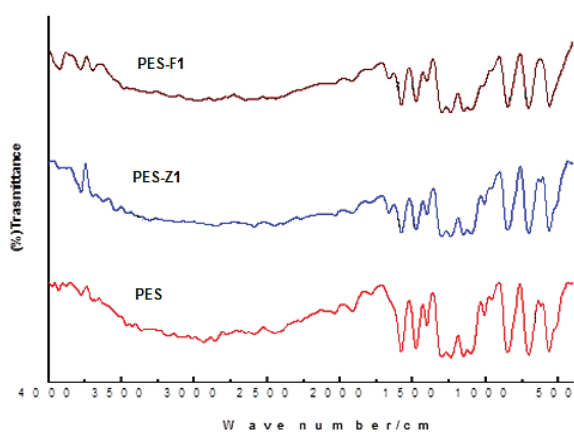


Fig. 7. FTIR spectrum of PES, PES, nZVI:Kaolin /PES (0.015 wt.%) and Fe:Kaolin/PES (0.015 wt.%) membranes.

are shown in Fig. 8. The nZVI:Kaolin and metallic Fe nanoparticles incorporated membranes showed more porous surface and sponge-like cross-section. Addition of nZVI:Kaolin and Fe:Kaolin in the PES dope has formed significant effect on both nZVI:Kaolin/PES and Fe:Kaolin/PES membranes in finger-like structure through large finger-like morphology and facilitated more sponge-like formation on bottom layer. In the surface morphology, virgin PES membrane has low porosity with pore sizes. The nZVI:Kaolin/PES membrane in addition of 0.5 wt % of nZVI:Kaolin nanoparticles showed a more porous skin with interconnected surface pore. In case of Fe:Kaolin/PES membrane, larger pores with distinctive pore size were observed through lower surface density. Even though, the obtained result is also supporting with Tauruzzi et al. [36] by incorporation of silver nanoparticles in to polysulfone nanocomposite membranes. From Fig. 8 it is clearly seen where the finger-like structure on both top skin and porous layer was reduced by adding of bimetallic Fe nanoparticles at 0.5 wt % in PES membrane. The change in morphology help an improved pore connectivity through the cross-section of membrane and metal loaded clay nanoparticles were visible on membrane surface. Diez et al. fabricated metal-doped mesostructured silica/polyethersulfone ultrafiltration membranes and reported the

visibility of metal loaded particles on PES surface [37]. The Fe metal on clay nanoparticles aggregates adsorbing or embedding in inner cross section and outer surface of the membrane when compared with virgin PES membrane. The clay minerals have the catalytic properties and the composite contain metal ions so the membrane might have good antifouling properties.

4.2.4. Hydrophilicity

From Table 1 the hydrophobic nature of PES membrane was changed to hydrophilicity with addition of different composition of nZVI:Kaolin and clay supported bimetallic Fe nanoparticles. The contact angle value of the nZVI:Kaolin/PES membranes were lesser than that of the virgin PES membrane. It also can be observed from the values that hydrophilicity of nZVI:Kaolin and bimetallic Fe nanoparticles incorporated PES membranes was increased while addition in different composition. This hydrophilicity enhancement of nZVI:Kaolin/PES and Fe:Kaolin/PES membranes are due to the higher affinity of clay nanoparticles [38] and metal loaded clay nanoparticles [39]. In general, clay minerals are hydrophilic in nature and incorporating organically and inorganically modified clays could exhibit well interaction between clay and polymer interface for better improvement in hydrophilicity. Anadão et al. reported that altering of morphology, hydrophilicity polysulfone (PSf) membrane by addition of Na montmorillonite clay (MMT) [40]. In this study, the hydrophilicity of the membrane was increased by increases of Na MMT content. The enhancement of hydrophilicity due to water sorption property, material's chemical structure and assistances in the wettability of membrane in the presence of kaolin nanoparticles. Moreover, the nZVI, Fe in kaolin modification was achieved by Fe reaction with Al_2O_3 , SiO_2 minerals which lead to the expansion of interlayer space of the clay in PES polymer. This clay layers enabled the intercalation of polymer macromolecules and dispersion of silicate layers in polymer matrix [41]. The enhance in hydrophilicity will favor to enhance the permeation flux of nZVI:Kaolin/PES and Fe:Kaolin/PES membranes.

4.2.5. Pure water flux

The pure water flux of PES, nZVI:Kaolin/PES and Fe:Kaolin/PES membranes at constant transmembrane pressure (TMP) was performed in different operating time (Fig. 9). The content TMP was chosen in 345 kPa because dead end ultrafiltration should perform in such a TMP. Initially, water flux was higher and flux value was declined and exhibited steady state value after 5 h continuous operation in dead end ultrafiltration. The membranes with higher initial fluxes experienced that lenient structure and incompatibility of membranes. However, initial fluxes of virgin PES membrane was less than the nZVI:Kaolin/PES and Fe:Kaolin/PES membranes and attained steady state value (flux profiles flattened) quickly. These lower fluxes showed that dense and small pore structure of PES membrane. Due increase hydrophilicity, pore size and sponge like structure by addition of nZVI:Kaolin/PES and Fe:Kaolin/PES membrane, the higher water flux was observed.

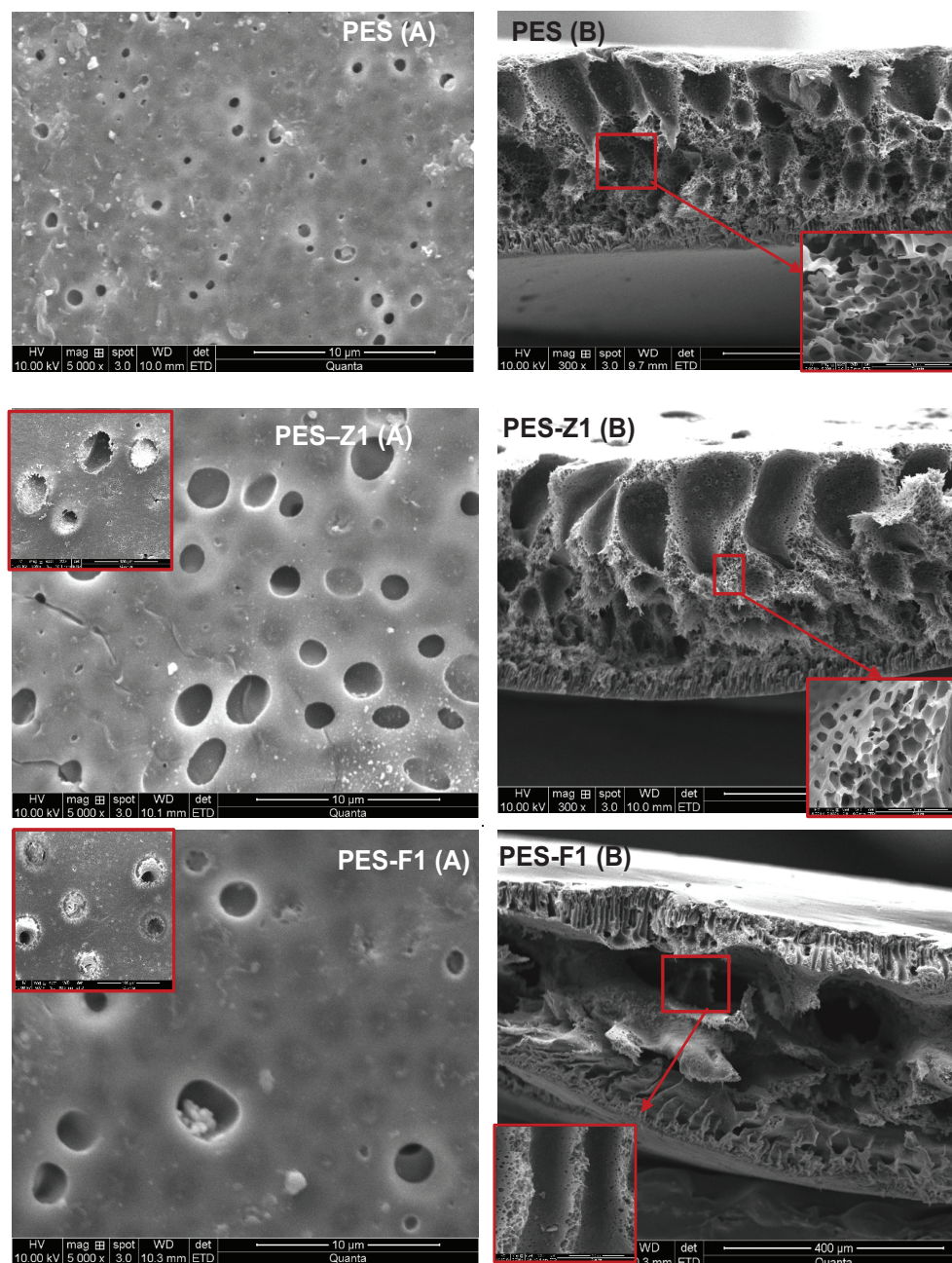


Fig. 8. Surface (A) and cross section (B) morphology of PES, PES, nZVI:Kaolin /PES (0.015 wt.%) and Fe:Kaolin/PES (0.015 wt.%) membranes.

4.2.6. Metal ion permeate flux

The permeate flux of metal ions like Cu(II), Ni(II), Cd(II) through PES, nZVI:Kaolin/PES and Fe:Kaolin/PES membranes in ultrafiltration is shown in Fig. 10. Fig. 10 shows the permeate flux of Cu(II), Ni(II), Cd(II) metal ions was increased for nZVI:Kaolin/PES and Fe:Kaolin/PES membranes. The increases in permeate flux by addition of various concentration of graphene oxide in polysulfone membrane was observed for metal ions [42]. The permeate flux for 0.030 wt. % of Fe:Kaolin in PES membranes was observed that higher predominated to comparison of

0.030 wt. % of nZVI:Kaolin/PES membrane which were confirmed that absence of Fe and in kaolin nanoparticles. However, the addition of 0.15 wt.% of nZVI:Kaolin and Fe:Kaolin nanoparticles enhanced the permeability which may be due to increase in hydrophilicity, pore size enhancement and alter in morphological structure. Fe₃O₄/montmorillonite nanocomposite (Fe₃O₄/MMT NC) was synthesized by Kalantari et al. [43] for removal of Pb²⁺, Cu⁺ and Ni²⁺ ions from aqueous systems. The Fe clay based nanomaterials was found to be best material for successful in removing heavy metals from their aqueous solutions. As a result, the

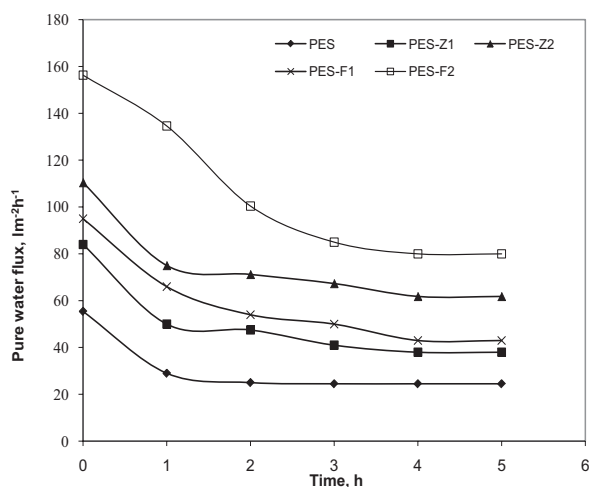


Fig. 9. Effect of operating time on pure water flux of PES, PES, nZVI:Kaolin/PES (0.015 wt.%) and Fe:Kaolin/PES (0.015 wt.%) membranes.

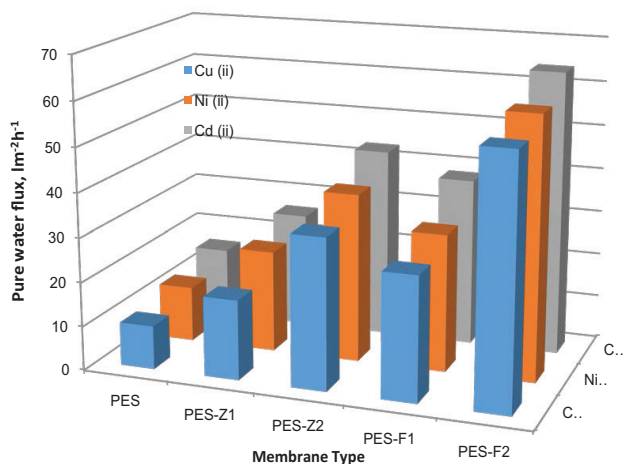


Fig. 10. Permeate flux of metal ions through PES, PES, nZVI:Kaolin/PES (0.015 wt.%) and Fe:Kaolin/PES (0.015 wt.%) membranes.

permeate flux of metal ions for all the membranes was in the following order of Cu(II) > Ni(II) > Cd(II).

4.2.7. Metal ions rejection

Fig. 11 shows metal ion rejections of the PES, nZVI:Kaolin/PES and Fe:Kaolin/PES membranes. The mechanisms of size exclusion (steric effect) and charge repulsion (Donnan exclusion) are contribute mainly in rejection on metal ions. The rejection is mainly due to steric effect which related to feed nature (radii of heavy metal ions), while the Donnan exclusion effect mostly depends on membrane properties (effect of clay nanoparticles on membrane surface). Here, nZVI and Fe present in kaolin was influenced the both synergic effect in/on PES membranes during metal ions separation. Gao et al. [44] reported the steric effect and Donnan exclusion on rejection of Pb(II), Cu(II),

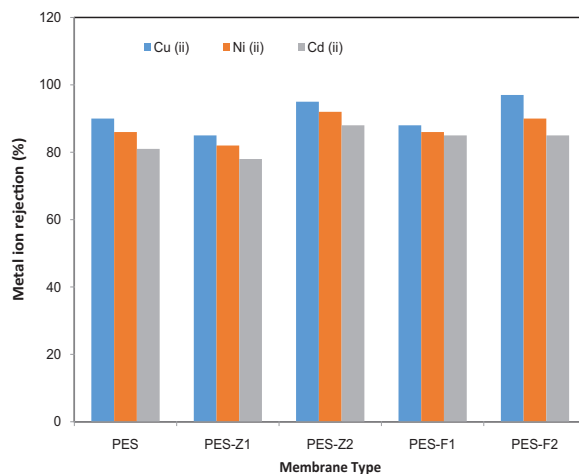


Fig. 11. Rejection of metal ions through PES, PES, nZVI:Kaolin/PES (0.015 wt.%) and Fe:Kaolin/PES (0.015 wt.%) membranes.

Ni(II), Cd(II) and Zi(II) metal ion using nanofiltration. The chosen heavy metal ions are the simple cations and have 2+ charges. The higher rejection of Cu(II) metal ions was observed for Fe:Kaolin/PES membrane and the order of metal ions rejection are Cu(II) (97%) < Ni(II) (90%) < Cd(II) (85%) depends on radii of three ions. The Fe₃O₄/talc nanocomposite was used for removal of Cu(II), Ni(II), and Pb(II) ions from aqueous solutions [45]. The PES membrane with nZVI:Kaolin nanoparticles had not present any metal (Fe) in the PES membrane, membranes are less pores on the surface, However, the radius of an ions are also related to diffusivity and permeability. Hence, the metal ion rejection of nZVI:Kaolin/PES membranes are lower when compare to Fe:Kaolin/PES membranes. The similar rejections were observed for heavy metals such as Cu(II), Ni(II) and Cd(II) when modified polymers ((poly (acrylic acid-co-maleic acid) (PAM), poly (acrylic acid) (PAA) and poly (dimethylamine-co-epichlorohydrin-co-ethylenediamine) (PDMED)) with polyethyleneimine (PEI) [46]. However, functionalized kaolin nanoparticles also influenced the rejection of metal ions can be improved significantly by increasing the nZVI:Kaolin and Fe:Kaolin nanoparticles in PES membrane.

5. Conclusions

The nano zerovalent iron-kaolin (nZVI:Kaolin) and metallic embedded kaolin clay nanoparticles was successfully synthesized. The appeared peak at 2θ of 56.55° was confirmed the formation of SiO₂. FTIR spectra and antimicrobial test were supported the presence of zerovalent iron and Fe²⁺ in kaolin clay nanoparticles. The nZVI:Kaolin nanoparticles was distributed on the kaolinite and iron oxide precursors was formed on the surface of nanoparticles. The analysis and characterization of nanoparticles confirmed that kaolin serves as modifier to alter PES membrane properties like hydrophilicity and morphology. In addition, the nZVI:Kaolin and Fe:Kaolin were well interacted with clay and PES for better improvement in hydrophilicity. The nZVI:Kaolin and Fe:Kaolin were influenced the forma-

tion sponge-like structure through large finger-like morphology in PES membranes. When 0.015 and 0.03 wt.% of nZV:Kaolin and Fe:Kaolin was added in PES, permeate flux of Cu(II), Ni(II), Cd(II) metal ions was increased. Further, nZV:Kaolin and Fe:Kaolin added in PES had better rejection of Cu(II), Ni(II), Cd(II) metal ions and enhanced the permeability which may be due to increase in hydrophilicity and change in morphological structure.

Acknowledgments

G. Arthanareeswaran acknowledges the Korean Federation of Science and Technology Society (KOFST) for the grant of Brain Pool Fellowship (161S-5-3-1561). The authors (GA, DBD and VJ) are also thankful to Royal Academy of Engineering, UK for Newton-Bhabha Higher Education Initiative Fund (Grant Number: HEP151642).

References

- M. Mulder, Basic Principles of Membrane Technology, Kluwer Academic Publishers, London, 1996.
- A. Rahimpour, S.S. Madaeni, Polyethersulfone (PES)/cellulose acetate phthalate (CAP) blend ultra filtration membranes: Preparation, morphology, performance and antifouling properties, *J. Membr. Sci.*, 305 (2007) 299–312.
- P.C. Sheng, Hydrophilic modification of poly (ethersulfone) ultrafiltration membrane surface by self-assembly of TiO₂ nanoparticles, *Appl. Surf. Sci.*, 249 (2005) 76–84.
- Y. Yanan, W. Peng, Preparation and characterizations of new PS/TiO hybrid membranes by sol–gel process, *Polymer*, 47 (2006) 2683–2688.
- Z.S. Wang, T. Sasaki, M. Muramatsu, Y. Ebina, T. Tanake, L. Wang, M. Watanabe, Self-assembled multilayers of titania nanoparticles and nanosheets with polyelectrolytes, *Chem. Mater.*, 15 (2003) 807–812.
- R. Molinari, M. Mungari, E. Drioli, A.D. Paola, V. Loddo, L. Palmisano, M. Schiavello, Study on a photocatalytic membrane reactor for water purification, *Catal. Today*, 55 (2000) 71–78.
- R. Molinari, C. Grande, E. Drioli, L. Palmisano, M. Schiavello, Photocatalytic membrane reactors for degradation of organic pollutants in water, *Catal. Today*, 67 (2001) 273–279.
- R. Molinari, L. Palmisano, E. Drioli, M. Schiavello, Studies on various reactors configurations for coupling photocatalysis and membrane process in water purification, *J. Membr. Sci.*, 206 (2002) 399–415.
- A. Bottino, G. Capannelli, V. D'Asti, Preparation and properties of novel organic–inorganic porous membranes, *Sep. Purif. Technol.*, 22 (2001) 269–275.
- A. Bottino, G. Capannelli, A. Comite, Preparation and characterization of novel porous PVDF–ZrO composite membranes, *Desalination*, 146 (2002) 35–40.
- L. Yan, Y.S. Li, C.B. Xiang, S. Xianda, Effect of nano-sized Al₂O₃-particle addition on PVDF ultrafiltration membrane performance, *J. Membr. Sci.*, 276 (2006) 162–167.
- D.J. Lin, C.L. Chang, F.M. Huang, L.P. Cheng, Effect of salt additive on the formation of microporous poly(vinylidene fluoride) membranes by phase inversion from LiClO₄/water/DMF/PVDF system, *Polymer*, 44 (2003) 413–422.
- N.M. Ismail, A.F. Ismail, A. Mustafaa, Sustainability in petrochemical industry: mixed matrix membranes from polyethersulfone/cloisite15A for the removal of carbon dioxide, *Procedia CIRP*, 26 (2015) 461–466.
- S. He, H. Jia, Y. Lin, H. Qian, J. Lin, Effect of clay modification on the structure and properties of sulfonated poly(ether ether ketone)/clay nanocomposites, *Poly. Compos.*, 37 (2016) 2632–2638.
- A.K. Zulkhairun, A.F. Ismail, T. Matsuura, M.S. Abdullah, A. Mustafa, Asymmetric mixed matrix membrane incorporating organically modified clay particle for gas separation, *Chem. Eng. J.*, 241 (2014) 495–503.
- R. Saranya, G. Arthanareeswaran, S. Sakthivelu, P. Manohar, Preparation and performance evaluation of nanokaolinite-particle-based polyacrylonitrile mixed-matrix membranes, *Ind. Eng. Chem. Res.*, 51 (2012) 4942–4951.
- O. Monticelli, A. Bottino, I. Scandale, G. Capannelli, S. Russo, Preparation and properties of polysulfone-clay composite membranes, *J. Appl. Polym. Sci.*, 103 (2007) 3637–3644.
- F. Bergaya, C. Detellier, J.F. Lambert, G. Lagaly, Introduction to clay polymer nanocomposites (CPN) Chapter 13, in: Lagaly, Bergaya (Eds.), *Handbook of Clay Science, Developments in Clay Science*. 2013, vol. 5A, Elsevier.
- P. Kilaris, C.D. Papaspyrides, Polymer/layered silicate (clay) nanocomposites: an overview of flame retardancy, *Prog. Polym. Sci.*, 35 (2010) 902–958.
- G. Rytwo, Clay minerals as an ancient nanotechnology: historical uses of clay organic interactions, and future possible perspectives, *Macla*, 9 (2008) 15–17.
- E. Petala, M. Baikousi, M.A. Karakassides, G. Zoppellaro, J. Filip, J. Tuček, K.C. Vasilopoulos, J. Pechouška, R. Zbořil, Synthesis, physical properties and application of the zero-valent iron/titanium dioxide heterocomposite having high activity for the sustainable photocatalytic removal of hexavalent chromium in water, *Phys. Chem. Chem. Phys.*, 18 (2016) 10637–10646.
- Y. Georgiou, K. Dimos, K. Beltsios, M.A. Karakassides, Y. Deligiannakis, Hybrid [polysulfone–Zero Valent Iron] membranes: Synthesis, characterization and application for AsIII remediation, *Chem. Eng. J.*, 281 (2015) 651–660.
- C. Liu, R. Bai, Adsorptive removal of copper ions with highly porous chitosan/cellulose acetate blend hollow fiber membranes, *J. Membr. Sci.*, 284 (2006) 313–322.
- H. Kaşgöz, A. Durmuş, A. Kaşgöz, Enhanced swelling and adsorption properties of AAm-AMPSNa/clay hydrogel nanocomposites for heavy metal ion removal, *Poly. Advan. Tech.*, 19 (2008) 213–220.
- R.S. Hebbar, A.M. Isloor, A.F. Ismail, Preparation and evaluation of heavy metal rejection properties of polyetherimide/porous activated bentonite clay nanocomposite membrane, *RSC Adv.*, 4 (2014) 47240–47248.
- E. Petala, K. Dimos, A. Douvalis, T. Bakas, J. Tucek, R. Zbořil, M.A. Karakassides, Nanoscale zero-valent iron supported on mesoporous silica: characterization and reactivity for Cr(VI) removal from aqueous solution, *J. Hazard. Mater.*, 261 (2013) 295–306.
- X. Wenga, Z. Chen, Z. Chen, M. Megharaj, R. Naidu, Clay supported bimetallic Fe/Ni nanoparticles used for reductive degradation of amoxicillin in aqueous solution: Characterization and kinetics, *Coll. Surf. A: Phys. Eng. Asp.*, 443 (2014) 404–409.
- F.S. Santos, F.R. Lago, L. Yokoyama, F.V. Fonseca, Synthesis and characterization of zero-valent iron nanoparticles supported on SBA-15, *J. Mater. Res. Technol.*, 598 (2017) 178–183.
- B.J. Saikia, G. Parthasarathy, Fourier transform infrared spectroscopic characterization of kaolinite from Assam and Meghalaya, Northeastern India, *J. Modern Phys.*, 1 (2010) 206–210.
- J.A. Gadsen, *Infrared Spectra of Minerals and Related Inorganic compounds*, Butterworths, London, 1975.
- Z.X. Chen, X.Y. Jin, Z.L. Chen, M. Megharaj, R. Naidu, Removal of methyl orange from aqueous solution using bentonite-supported nanoscale zero-valent iron, *J. Colloid Interface Sci.*, 363 (2011) 601–607.
- K.A. Carrado, Synthetic organo- and polymer-clays: preparation, characterization, and materials applications, *Appl. Clay Sci.*, 17 (2000) 1–23.
- T. Wu, A.G. Xie, S.Z. Tan, X. Cai, Antimicrobial effects of quaternary phosphonium salt intercalated clay minerals on *Escherichia coli* and *Staphylococcus aureus*, *Coll. Surf. B: Biointer.*, 86 (2011) 232–236.

- [34] B. Deng, X. Yang, L. Xie, J. Li, Z. Hou, S. Yao, G. Liang, K. Sheng, Q. Huang, Microfiltration membranes with pH dependent property prepared from poly(methacrylic acid) grafted polyethersulfone powder, *J. Membr. Sci.*, 330 (2009) 363–368.
- [35] X. Wang, P. Liu, J. Ma, H. Liu, Preparation of novel composites based on hydrophilized and functionalized polyacrylonitrile membrane-immobilized NZVI for reductive transformation of metronidazole, *Appl. Surf. Sci.*, 396 (2017) 841–850.
- [36] J.S. Taurozzi, H. Arul, V.Z. Bosak, A.F. Burban, T.C. Voice, M.L. Bruening, V.V. Tarabara, Effect of filler incorporation route on the properties of polysulfone–silver nanocomposite membranes of different porosities, *J. Membr. Sci.*, 325 (2008) 58–68.
- [37] J.C. Mierzwa, V. Arieta, M. Verlage, J. Carvalho, C.D. Vecitis, Effect of clay nanoparticles on the structure and performance of polyethersulfone, *Desalination*, 314 (2013) 147–158.
- [38] N. Bouazizi, D. Barrimo, S. Nouisir, R. Ben Slama, T.C. Shiao, R. Roy, A. Azzouz, Metal-loaded polyol-montmorillonite with improved affinity towards hydrogen, *J. Energy Instit.*, 91 (2018) 110–119.
- [39] B. Díez, N. Roldán, A. Martín, A. Sotto, P.J.A. Melón, J. Arsuaga, R. Rosala, Fouling and biofouling resistance of metal-doped mesostructured silica/polyethersulfone ultrafiltration membranes, *J. Membr. Sci.*, 526 (2017) 252–263.
- [40] P. Anadão, L.F. Sato, R.R. Montes, S. Henrique, D. Santis, Polysulphone/montmorillonite nanocomposite membranes: Effect of clay addition and polysulphone molecular weight on the membrane properties, *J. Membr. Sci.*, 45 (2014) 187–199.
- [41] A. Okada, A. Usuki, The chemistry of polymer–clay hybrids, *Mater. Sci. Eng. C.*, 3 (1995) 109–115.
- [42] R. Mukherjee, P. Bhunia, S. De, Impact of graphene oxide on removal of heavy metals using mixed matrix membrane, *Chem. Eng. J.*, 292 (2016) 284–297.
- [43] K. Kalantari, M.B. Ahmad, H.R.F. Masoumi, K. Shameli, M. Basri, R. Khandanlou, Rapid and high capacity adsorption of heavy metals by Fe_3O_4 /montmorillonite nanocomposite using response surface methodology: Preparation, characterization, optimization, equilibrium isotherms, and adsorption kinetics study, *J. Taiwan Instit. Chem. Eng.*, 49 (2015) 192–198.
- [44] J. Gao, S.P. Sun, W.P. Zhu, T.S. Chung, Chelating polymer modified P84 nanofiltration (NF) hollow fiber membranes for high efficient heavy metal removal, *Water Res.*, 63 (2014) 252–261.
- [45] K. Kalantari, M. Ahmad, H. Masoumi, K. Shameli, M. Basri, R. Khandanlou, Rapid adsorption of heavy metals by Fe_3O_4 /talc nanocomposite and optimization study using response surface methodology, *Int. J. Mol. Sci.*, 15 (2014) 12913–12927.
- [46] G. Arthanareeswaran, V.M. Starov, Effect of solvents on performance of polyethersulfone ultrafiltration membranes: investigation of metal ion separations, *Desalination*, 267 (2011) 57–63.